PIBB 生物化学与生物物理进展
Progress in Biochemistry and Biophysics
2021,48(8):966~972
www.pibb.ac.cn

Four-focus Switch Optical Coherence Tomography for Whole Eye Segment Imaging and Visual Axis Parameters Measurement*

LUO Jia-Xiong**, LI Jian-Cong**, YU Miao, GUAN Cai-Zhong, HUANG Li-Yuan, ZENG Ya-Guang, WU Yan-Xiong***
(*School of Physics and Optoelectronic Engineering, Foshan University, Foshan* 528000, China)

Abstract We demonstrate the feasibility of a four-focus switch Fourier-domain optical coherence tomography system for whole eye segment imaging, and *in vivo* visual axis parameter (VAP) measurement. In this study, we use two rotating disks to switch the focus position synchronously, to expand the detection depth range. Three parallel glass plates of different thicknesses are placed on a rotating disk along the path of the detection beam, so as to switch the focus position of the probing beam from the cornea, the anterior and posterior of the lens to the retina. On the other synchronously rotating disk, the light path of the reference arm can simultaneously extend the detecting optical path to match the probing beam. This multistage focusing method can make the probing beam completely focused on each segment of the human eye during the course of signal collection. Subsequently, we measured VAP several times, and the results show that our four-focus switch FD-OCT system exhibits good repeatability. In conclusion, we prove theoretically and experimentally that the proposed four-focus switched FD-OCT system can realize whole eye segment imaging and VAP measurement, including central corneal thickness, anterior chamber depth, lens thickness, and axial length. Our method will be beneficial for measurements in ophthalmology.

Key words optical coherence tomography, whole eye segment imaging, visual axis parameters
DOI: 10.16476/j.pibb.2020.0390

Accurate measurements of all visual axis parameters (VAP) are prerequisites for studying the development of refractive errors in human eyes, which is critical for cataract surgery. Significant VAPs include the central corneal thickness (CCT), anterior chamber depth (AD), lens thickness (LT), and axial length (AL). For a normal human eye, the measurement of these parameters ranges from 25 to 35 mm in air. Some non-contact optical methods are being developed to make *in vivo* measurements of VAPs[1-3]. For example, there are two types of devices that are available for measuring human eyes: IOL-Master (Meditec, Carl Zeiss, Jena, Germany) and Lenstar LS900 (HaagStreit AG, CH-3098 Koeniz, Switzerland). IOL master is the first commercial optical biometer launched in 1999. In cataract surgery, it is widely used as the standard of intraocular lens selection[4]. The Lenstar LS900 is a kind of non-invasive biological measurement instrument with optical low coherence reflectometer (OLCR), which has been widely used in the market[5]. Recently, Pentacam-AXL (Oculus, Germany), by using partial coherence interferometry technology to obtain the measurement of AL, and obtained the ability of non-contact biometry[6]. These above devices were originally developed from time-domain low coherence interferometry. Although the above optical biometers based on time-domain low coherence interferometry provide higher resolution than ultrasound, their application is limited due to the penetration of light. Owing to high speed and

* This work was supported by grants from The National Natural Science Foundation of China (11474053, 11204037, 61307062).
** These authors contributed equally to this work.
*** Corresponding author.
Tel: 86-18943994810, E-mail: winsword@sina.com
Received: October 29, 2020 Accepted: March 9, 2021

sensitivity, it is well accepted that frequency-domain optical coherence tomography (FD-OCT) is more suitable for ophthalmic measurements. For example, the OA-2000 is a biometer based on Fourier domain technology by light interference using a swept-source laser. Swept-source optical coherence tomography is a relatively new technique of Fourier domain OCT with better penetrability[7]. But as the device use frequency sweeping technology, the introduction of mechanical devices will also reduce the stability of the system and the system is very expensive. Therefore, realizing whole eye segment imaging and measuring VAPs simultaneously, using the same FD-OCT system, is a challenging task. The maximal measurement depth range of an FD-OCT system is limited by the spectrometer resolution, which typically lies in the approximate range of 1−5 mm, for state-of-the-art systems. The other major limitation is that, owing to the refractive power of the anterior segment, a probing beam cannot be focused on the anterior and posterior segments of the eye simultaneously. Therefore, a common FD-OCT system is not sufficient for whole eye imaging and VAP measurement. Consequently, efforts have been made to extend the ranging capability and control the focus position of the probing beam simultaneously. A typically adopted solution is to use a dual arm configuration[8-11]. The probing beam is split in two, and focused on the anterior segment and retina. Two independent and separated reference arms are used to match the optical paths of the two probing beams. The measurement scheme can be viewed as a combination of two FD-OCT systems, where the probing beam for the anterior segment requires a high depth of field lens to focus on the cornea and lens simultaneously.

In this study, we propose a four-focus switch FD-OCT system for whole eye segment imaging and *in vivo* VAP measurements. Two rotating disks are used to synchronously switch the focus position and extend the detection depth range. Three parallel glass plates are placed on a rotating disk along the path of the probing beam, to sequentially switch the focus position from the cornea and the anterior and posterior of the lens to the retina. On the other synchronously rotating disk, the light path of the reference arm can simultaneously extend the detecting optical path to match the probing beam. Contrary to previous studies, we used only one FD-OCT system to realize independent segment images of the cornea, lens, and retina. In addition, we measured CCT, AD, LT, and AL. An added advantage of this multistage focusing method is that the probing beam can be completely focused on each segment of the human eye during the course of signal collection.

1 Materials and methods

As shown in figure 1a, the optical path can be extended by inserting a parallel glass plate into the parallel reference beam[12]. The increased optical path length ΔL can be expressed as:

$$\Delta L = d_0\left(n_0 - 1\right) \tag{1}$$

where d_0 and n_0 are the thickness and refractive index of the inserted parallel glass plate, respectively. This method can be used to extend the detection range from the cornea to the lens in our experiment. Moreover, a parallel glass plate is used to change the focusing position by inserting it into the converging optical path of the probing beam (Figure 1b). The shifted distance ΔP can be evaluated from the principles of geometrical optics as:

$$\Delta P = d_0\left(1 - \frac{\cos\theta}{\sqrt{{n_0}^2 - \sin^2\theta}}\right) \tag{2}$$

where θ is the angle of incidence. For the OCT image, the probing beam diameter and scan angle of the galvanometer are relatively small. The OCT image can be viewed as a paraxial condition, *i.e.*, $\theta \approx 0$, $\sin\theta \approx 0$, and $\cos\theta \approx 1$. Then, the shifted distance PP' of the focus spot can be presented approximately as:

$$\Delta P = d_0\left(1 - \frac{1}{n_0}\right) \tag{3}$$

The above theory is applied to develop a four-focus switch FD-OCT system. Figure 2 shows a four-focus switch optical schematic for changing the focus of the probing beam from the cornea and lens to the retina. In our experimental setup, the equivalent focal lengths of the probing optical system are 30 mm (lens L1) and 20 mm (lens L2). The distance between L1 and L2 is 55 mm. The work distance from lens L2 to the surface cornea is approximately 100 mm. Then, the probing beam is first focused at the cornea (figure 2a). For a normal human eye model, the average statistical lengths of AD and LT are approximately 3.15 mm and 3.75 mm, respectively[13]. To change the focus from the cornea to the anterior and posterior of the lens according to equation (2) and the Gaussian

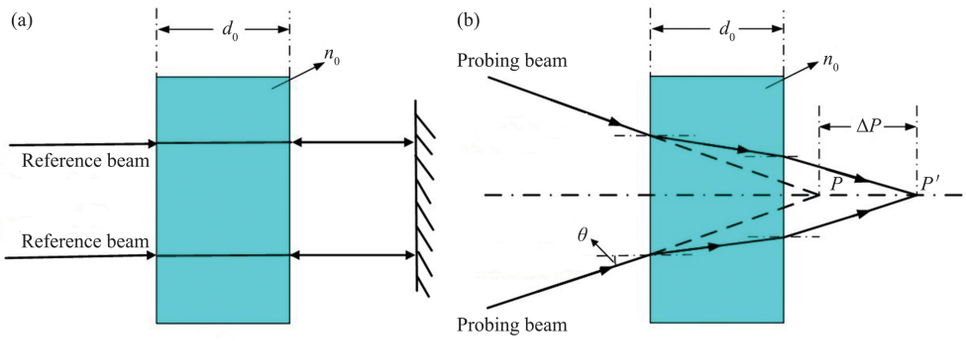

Fig. 1　The principle of parallel glass plate used to extend optical path and change focus position

(a) Extension of the optical path for the reference beam. (b) Focus switch for the probing beam inserting a parallel glass plate.

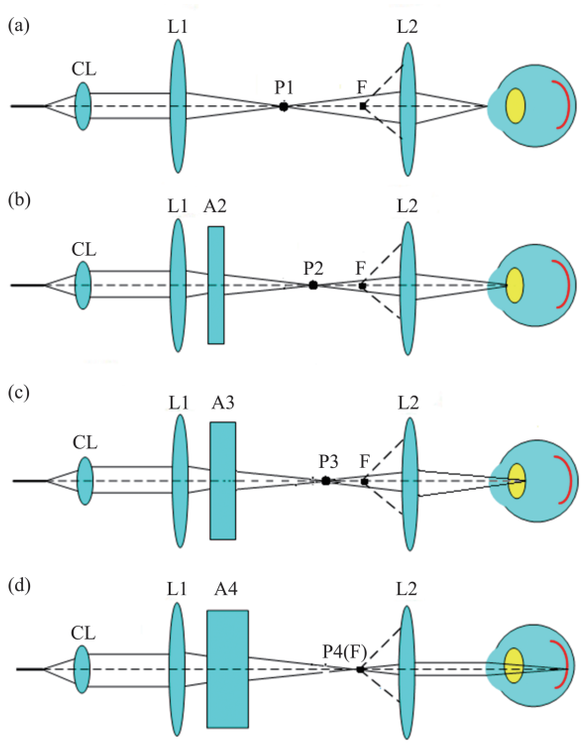

Fig. 2　The four−focus switch optical schematic for changing the focus of the probing beam from the cornea to the retina

Schematic of the four-focus switch optical probing beam from the (a) cornea, (b) anterior and (c) posterior of lens, and (d) retina. A2−4: Inserted parallel glass plates, CL: Collimator, P1−4: The focus of lens L1 without parallel glass plate and with different thickness of parallel glass plate, F: The focus of lens L2.

imaging formula, the thicknesses of the inserted glass A2 and A3 (K9, n_0=1.51 at 850 nm) are approximately 0.95 mm and 1.85 mm, respectively (Figure 2b, c). When the focus of the probing beam is shifted to the retina, P4 should overlap with focus F of L*2* (Figure 2d). The thickness of the inserted glass A4 is 8.32 mm in this case (ZnSe, n_0=2.51 at 850 nm).

Figure 3a shows a schematic of the four-focus FD-OCT system. A superluminecent diode (SLD; Superlum Ltd) light source has a central wavelength of 840 nm and bandwidth of 64 nm, with an axial resolution of 4.7 μm in air. The beam from the SLD was split into the probing beam and reference beam by fiber couple 1. The optical power of the probing beam was set to ~0.68 mW, which meets the safety requirements for continuous illumination according to eye safety standards[14]. The reference beam was split into two arms (reference beam 1 and reference beam 2) to match the optical path of the probing beam by fiber couple 2. The light emerging at the output of the interferometer was sent to a homebuilt high-speed spectrometer that employed a line-scan camera (SPL2048-140km, Basler) to capture the interferograms formed in the system. The data acquisition frequency of the linear camera in this system was set to 100 kHz by reducing the number of redundant pixels. The spectrometer had a designed image depth of 2.5 mm in air. A color camera in the probing beam path was used to help the operator monitor the eye surface using a dichroic mirror. To continuously shift the focus and extend the detection depth, two rotating disks, D1 and D2, were designed to switch different inserted parallel glass plates (Figure 3b). D1 and D2 are simultaneously driven by a servo motor with a synchronous belt (Figure 3c). Disk D1, with four optical windows, is used to shift the focus of the probing beam on the cornea (A1, without parallel glass plate), anterior (A2) and posterior (A3) surface of the lens, and retina (A4). The thicknesses of the inserted parallel glass plates A2, A3, and A4 are analyzed in Figure 2. Near the centers of windows A1 to A4, four windows T were designed to trigger VAP

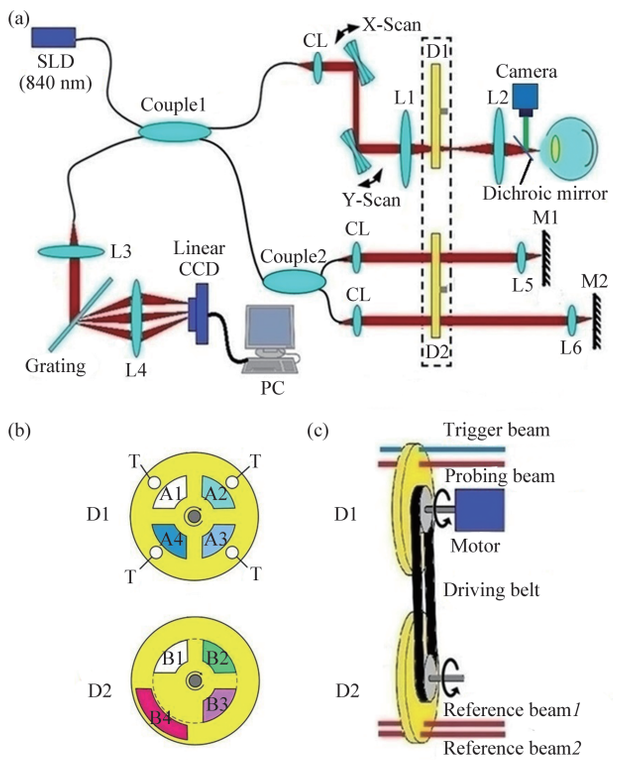

Fig. 3　The principle of four−focus switch FD−OCT system

(a) Schematic of the four-focus switch FD-OCT system. (b, c) Two synchronous rotating disks D1 and D2. A1, B1, B4, T: Hole; A2−4, B2−3: Inserted parallel glass plates, CL: Collimator; L1−6: Lens; M1, 2: Mirror.

measurement and localize the servo motor for the OCT image at the corresponding position, where a laser diode (650 nm) and photodiode are used to generate the trigger signal. The other disk D2 with four windows (B1 to B4) was used to match different detection depths. B1 had no parallel glass plate inserted into the optical path of reference beam *1*, which corresponds to the case of the focus of the probing beam at the cornea. When the focus of the probing beam was shifted to the anterior and posterior surfaces of the lenses, the thicknesses of B2 and B3 inserted into the optical path of reference beam *1* were approximately 4.53 mm and 8.37 mm (ZnSe, n_0=2.51 at 850 nm), respectively, based on equation (1). When the probing beam was shifted to the retina, reference beam *2* was separated to a greater extent to match the optical path of the probing beam. To avoid confusion regarding the reference beams, window B4 without a parallel glass plate had a different diameter than the other three windows. The advantage of this design is that only one reference beam can be reflected and interfered with the probing beam from the corresponding position. All inserted parallel glass plates were coated with an antireflective film to examine the loss of light detection. The dispersion compensation parameters were individually calibrated for different inserted parallel glass plates[15].

2　Experiments and results

In the signal-acquired processing of OCT segment imaging, the computer accurately controls the servo motor to retain the position of one segment. Different driving voltages on the galvanometer were used to control the B-scan range, and OCT sectional images of different segments were obtained. Figure 4 shows the sectional OCT image of a normal human eye of a male volunteer, including the cornea (Figure 4a), anterior and posterior surfaces of the lens (Figure 4b, c), and retina (Figure 4d), where every B-scan frame includes a 1 000 A-scan line. Figure 4b shows that the cortex lay of the lens is apparent, and the strong reflective line (Figure 4c), demonstrates that the probing beam is focused on the posterior surface of the lens. This result shows that the four-focus FD-OCT system is sensitive to whole eye segment imaging, owing to the multistage focusing method.

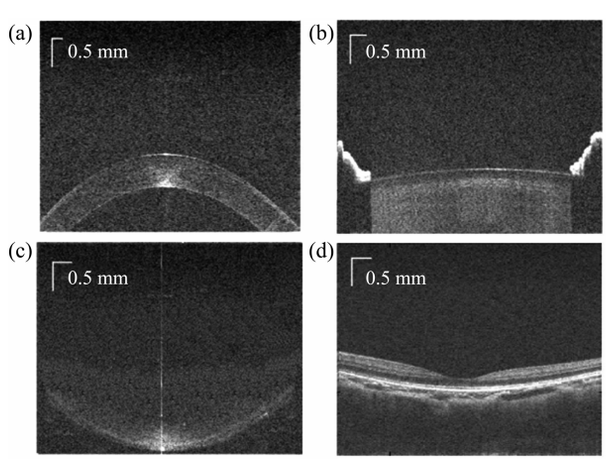

Fig. 4　The sectional OCT image of the normal human eye

OCT cross sectional image of the (a) cornea, (b) anterior and (c) posterior of the lens, and (d) retina.

In the VAP measurement, the rotating speed of the servo motor was set to 600 r/min, the single acquisition time is about 0.1 s, which ensured that the eye was immobile during every signal acquisition in the normal condition. The linear camera was triggered

to record 30 A-scan lines at every trigger position T on disk D1. The axial motion between adjacent A-lines was eliminated with the correlation-based and phase compensation algorithm[15], which ensures that the peak of every A-scan line is averaged accurately. Four averaged signals from the cornea, anterior and posterior surface of the lens, and retina were recombined with the interval distance shifted by the inserted parallel glass plates. The interval distance shifted by the inserted parallel glass plate was measured using an optical grating ruler (KA300, Nuoxin) with a resolution of 0.2 μm[16]. Figure 5 shows a typical *in vivo* VAP signal of the human eye. To simplify the VAP signal processing, a signal threshold (2.85 in this study) was set to remove the background. A Labview peak searching algorithm was used to determine the boundary signal (*A*, *B*, *C*, *D*, and *E*) of the entire eye[17]. Among them, *A* and *B* represent the corneal, *C* and *D* represents the anterior and posterior parts of the lens respectively, and *E* represents the retina. The parameters, *i.e.*, CCT, AD, LT, and AL, correspond to the distance of *AB*, *BC*, *CD*, and *AE*, which are obtained using the measured optical paths to divide their corresponding refractive indices. The results of three successful experiments according to Lenstar's signal processing method are presented in Table 1. The results show that the standard deviation of the three measurements of CCT is 2.1 μm, and the standard deviation of AD, LT and AL is less than 40 μm. These measurement data show that our four-focus switch FD-OCT system exhibits good reproducibility.

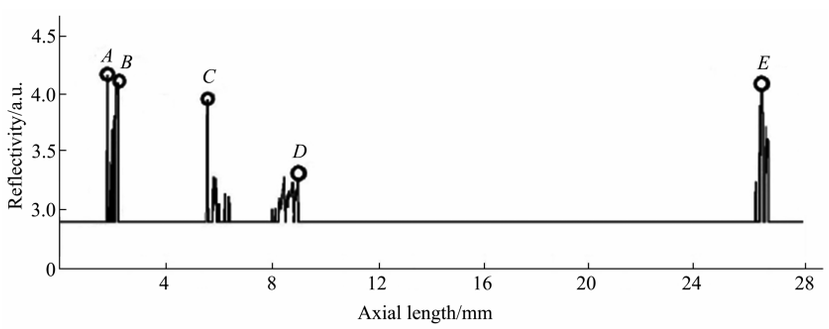

Fig. 5 *In vivo* VAP signal of the human eye

VAP signal created by recombining four averaged A-scan signals of the (*A*, *B*) cornea, (*C*) anterior and (*D*) posterior of the lens, and (*E*) retina with the interval distance of the inserted parallel glass plates.

Table 1 VAP measurement of the human eye

Measurement	CCT/μm	AD/mm	LT/mm	AL/mm
1	542	3.30	3.63	25.10
2	546	3.32	3.58	25.08
3	545	3.33	3.60	25.03
Mean	544	3.32	3.60	25.07
SD	2.1	0.02	0.025	0.036

3 Discussion and conclusion

Although our four-focus switch FD-OCT system has realized segment imaging and VAP measurement, there exist some issues that need to be addressed. The focal length of the probing beam for the retina is different for myopic or presbyopic eyes. Thus, the focus at the retina should be adjustable for different people. A possible solution is to combine the parallel glass plate A4 with a liquid lens on D1, in which the focal length can be accurately driven by an externally controlled voltage. A precision translation will be considered to synchronously adjust the reflection position of reference beam 2. To realize a practical measurement system, each inserted parallel glass plate should be fixed on the same rotating disk, where different parallel glass plates have different radii. The optical system of the probing light should be further carefully optimized to eliminate the field curvature of the inserted parallel glass plate. A fixation system should also be developed for practical applications, because it is difficult for patients to concentrate on the light spot for longer periods of time.

In summary, our preliminary experiment shows that the proposed four-focus switching FD-OCT

system is sensitive to the whole eye segment imaging due to the multistage focusing method, which can realize segment imaging of the whole eye and simultaneously measure VAPs, including CCT, AD, LT and AL. Our method will be beneficial for measurements in ophthalmology.

References

[1] Fercher A F, Mengedoht K, Werner W. Eye-length measurement by interferometry with partially coherent light. Optics Letters, 1988, **13**(3): 186-188

[2] Grulkowski I, Gora M, Szkulmowski M, *et al*. Anterior segment imaging with Spectral OCT system using a high-speed CMOS camera. Optics Express, 2009, **17**(6): 4842-4858

[3] Chong C, Suzuki T, Totsuka K, *et al*. Large coherence length swept source for axial length measurement of the eye. Applied Optics, 2009, **48**(10): 144-150

[4] Santodomingo-Rubido J, Mallen E A H, Gilmartin B, *et al*. A new non-contact optical device for ocular biometry. British Journal of Ophthalmology, 2002, **86**(4): 458-463

[5] Cruysberg L P J, Doors M, Verbakel F, *et al*. Evaluation of the Lenstar LS 900 non-contact biometer. Br J Ophthalmol, 2010, **94**(1): 106-110

[6] Khoramnia R, Rabsilber T M, Auffarth G U. Central and peripheral pachymetry measurements according to age using the Pentacam rotating Scheimpflug camera. Journal of Cataract & Refractive Surgery, 2007, **33**(5): 830-836

[7] Huang J, Savini G, Hoffer K J, *et al*. Repeatability and interobserver reproducibility of a new optical biometer based on swept-source optical coherence tomography and comparison with IOLMaster. British Journal of Ophthalmology, 2017, **101**(4): 493-498

[8] Shao Y, Tao A, Jiang H, *et al*. Simultaneous real-time imaging of the ocular anterior segment including the ciliary muscle during accommodation. Biomedical Optics Express, 2013, **4**(3): 466-480

[9] Jeong H W, Lee S W, Kim B M. Spectral-domain OCT with dual illumination and interlaced detection for simultaneous anterior segment and retina imaging. Optics Express, 2012, **20**(17): 19148-19159

[10] Dai C, Zhou C, Fan S, *et al*. Optical coherence tomography for whole eye segment imaging. Optics Express, 2012, **20**(6): 6109-6115

[11] Kim J H, Moon T H, Chae J B, *et al*. Measurement reliability of axial length of the human eye by using partial coherence interferometry. Journal of the Optical Society of Korea, 2014, **18**(5): 546-550

[12] Pedersen C J, Huang D, Shure M A, *et al*. Measurement of absolute flow velocity vector using dual-angle, delay-encoded Doppler optical coherence tomography. Optics Letters, 2007, **32**(5): 506-508

[13] He J C, Gwiazda J, Thorn F, *et al*. Wave-front aberrations in the anterior corneal surface and the whole eye. J Opt Soc Am A Opt Image Sci Vis, 2003, **20**(7): 1155-1163

[14] Lavery I. Safe use of lasers. Occup Health, 1978, **30**(5): 220-222

[15] Ma, Zhenhe. Practical approach for dispersion compensation in spectral-domain optical coherence tomography. Optical Engineering, 2012, **51**(6): 3203-3211

[16] Grajciar B, Pircher M, Hitzenberger C K, *et al*. High sensitive measurement of the human axial eye length *in vivo* with Fourier domain low coherence interferometry. Optics Express, 2008, **16**(4): 2405-2414

[17] Makita S, Hong Y, Yamanari M, *et al*. Optical coherence angiography. Optics Express, 2006, **14**(17): 7821-7840

用于全眼段成像和视轴参数测量的四焦点开关光学相干断层扫描*

罗佳雄** 李建聪** 余　苗　关财忠　黄丽媛　曾亚光　伍雁雄***

（佛山科学技术学院物理与光电工程学院，佛山 528000）

摘要　本文演示了四焦点开关傅里叶域光学相干断层扫描系统用于全眼段成像和体内视轴参数（VAP）测量的可行性. 使用包括不同厚度平行玻璃板的两个同步转盘来将探测光束的焦点位置从角膜以及晶状体的前部和后部切换到视网膜. 该过程同时增加了参考光束的深度范围. 这种多级聚焦的方法可以使探测光束完全聚焦在人眼的每个部分. 初步实验表明，该方法可以实现全眼段成像和包括中央角膜厚度、前房深度、晶状体厚度和轴长在内的VAP测量.

关键词　光学相干断层扫描，全眼段成像，视轴参数

中图分类号　O445　　**DOI**：10.16476/j.pibb.2020.0390

* 国家自然科学基金（11474053、11204037、61307062）资助项目.

** 并列第一作者.

*** 通讯联系人.

Tel：18943994810，E-mail：winsword@sina.com

收稿日期：2020-10-29，接受日期：2021-03-09